Journal of Sound and Vibration 356 (2015) 61–71

Contents lists available at ScienceDirect

Journal of Sound and Vibration

journal homepage: www.elsevier.com/locate/jsvi

Damping loss factor estimation of two-dimensional orthotropic structures from a displacement field measurement

Raef Cherif [a,*], Jean-Daniel Chazot [b], Noureddine Atalla [a]

[a] GAUS, University of Sherbrooke, Sherbrooke (Québec), Canada J1K 2R1
[b] Sorbonne universités, Université de technologie de Compiègne, CNRS, laboratoire Roberval UMR 7337, 60203 Compiègne Cedex, France

ARTICLE INFO

Article history:
Received 27 December 2014
Received in revised form
1 June 2015
Accepted 26 June 2015
Handling Editor: I. Lopez Arteaga
Available online 21 July 2015

ABSTRACT

This paper presents a damping loss factor estimation method of two-dimensional orthotropic structures. The method is based on a scanning laser vibrometer measurement. The dispersion curves of the studied structures are first estimated at several chosen angles of propagation with a spatial Fourier transform. Next the global damping loss factor is evaluated with the proposed inverse wave method. The method is first tested using numerical results obtained from a finite element model. The accuracy of the proposed method is then experimentally investigated on an isotropic aluminium panel and two orthoropic sandwich composite panels with a honeycomb core. The results are finally compared and validated over a large frequency band with classical methods such as the half-power bandwidth method (3 dB method), the decay rate method and the steady-state power input method. The present method offers the possibility of structural characterization with a simple measurement scan.

1. Introduction

The reduction of structural vibrations is a remaining challenge in aircraft design where damping treatments, such as constrained viscoelastic layers or damping patches[1], are widely used to reduce resonant vibrations [2–6]. Various experimental techniques have hence been developed over the years to characterize the performance of damping treatments. The most known are the half-power bandwidth method (3 dB method) [7], the decay rate method [8,9] and the steady-state power input method [9], but other methods can also be cited such as the Oberst beam method [10], the Bayesian method [11] based on a numerical multilayer model [12], the Force Analysis Technique [13] also known by the French acronym RIFF method.

Recently, a wave approach has been used by McDaniel et al. in Ref. [14] to estimate frequency-dependant loss factors in one-dimensional structures. In this work, a few number of accelerometers are placed on a beam to identify the complex wavenumbers of flexural and evanescent waves at each frequency. The damping loss factor is then related to the imaginary part of the estimated wavenumber. This approach uses a nonlinear optimization algorithm that minimizes the error between the measured responses and the wave model by adjusting the complex wavenumbers and amplitudes. On the other hand, the wavenumber identification of propagating waves in two-dimensional structures has also been studied [15–23]. Among these works, Ferguson et al. [15] proposed a method to evaluate the correlation between normal velocity

* Corresponding author.
E-mail address: raef.cherif@usherbrooke.ca (R. Cherif).

http://dx.doi.org/10.1016/j.jsv.2015.06.042
0022-460X/

measurements in the complex domain and a wavefield $e^{jk_x x}e^{jk_y y}$. This correlation method is however limited at one unique dominant wavenumber without damping. Another wavenumber identification method based on Prony series was tested by Grosh et al. in Ref. [16]. This numerical work also did not take into account the structural damping and was not applied to experimental data. Recently, Berthaut et al. [17] proposed an inhomogeneous wave correlation method similar to Ferguson's method. The difference in their work is to correlate the measurements with an inhomogeneous wave field that takes into account damped waves. Ichchou et al. used the same inhomogeneous wave correlation method to identify the guided waves propagating in ribbed panels in Refs. [18,19], and to identify the flexural wavenumber in composite structure with honeycomb cores in Ref. [20]. Finally, Rak et al. showed in Ref. [21] that the inhomogeneous wave correlation method was not adapted to estimate the structural loss factor compared to the McDaniel method. Halkyard arrived to the same conclusions in Ref. [22] with his maximum likelihood method applied to lightly damped plates.

Despite this rich literature, practitioners are still struggling to identify the damping loss factor of two-dimensional structures. In this context, the case of complex panels with damping has not yet been treated.

A recent article by Cherif and Atalla [24] discusses in detail the measurement vs predictions of different vibroacoustic indicators of two composite sandwich panels (wavenumbers, radiation efficiency, modal density, damping loss and transmission loss). In particular, the use of the wavenumber measurement to estimate the modal density and the radiation efficiency is discussed. However, the estimation of the damping loss factor from the wavenumber measurement is still a missing task. The purpose of this paper is to overcome the limitation met in the above-mentioned works and offers the possibility of a full structural characterization of two-dimensional orthotropic structures with a simple measurement scan to estimate the wavenumbers, the radiation efficiency, the modal density, the global damping loss factor and the transmission loss.

This paper presents a damping loss factor estimation method of two-dimensional structures from a displacement field measured with a scanning laser vibrometer. Based on the inhomogeneous wave correlation, the orthotropic dispersion curves are obtained at each angle of propagation θ and the related damping loss factors are estimated at the same angles. The accuracy of the proposed method is investigated on numerical results obtained with a finite element model and then on experimental data. For the latter a metallic panel and two sandwich composite panels with honeycomb cores are tested. The present method is then compared to classical methods such as the 3 dB method, the decay rate method and the power input method. The analysis is performed over a large frequency range from 100 Hz to 10 kHz.

2. Inverse wave method

This section outlines the proposed inverse wave method used to estimate the damping loss factor of complex two dimensional structures.

In Ref. [17] the inhomogeneous wave correlation technique is presented and employed to identify the real and imaginary parts of complex wavenumbers in two dimensional structures at a given angle of propagation θ. This is a difficult task since the loss factor values are very small and sensitive to the wavenumber amplitudes.

To overcome this limitation, the proposed method uses first the inhomogeneous wave correlation technique detailed in Refs. [17–20] to identify accurately the dispersion curve. Then the estimated wavenumber amplitude is used as an input value in the inhomogeneous wave correlation technique to obtain a reliable estimation of the loss factor. The influence of the measurement noise on the identification process is also taken into account by the introduction of the coherence function in the inhomogeneous wave correlation (see Ref. [21]).

The proposed method assumes a harmonic field $\hat{w}(x,y)$, either from a harmonic excitation or from a temporal Fourier transform. The dependence in ω is simply denoted with a hat. The displacement field $\hat{w}(x_p,y_q)$ is measured over a uniform grid ($x_p = p\Delta x, y_q = q\Delta y$) with $1 \le p,q \le N$, and Δx and Δy the space increments along the x- and the y-axis respectively. Here the same number N of measured data along the x- and the y-axis is taken, but this is not a limitation of the method. Outside this grid a baffle condition is considered. The displacement is written in the wavenumber domain with the classical spatial discrete Fourier transform calculated over a domain $l_x \times l_y$ not necessarily equal to the panel area $L_x \times L_y$:

$$\hat{W}(k_x,k_y) = \frac{l_x l_y}{N^2}\sum_{p=1}^{N}\sum_{q=1}^{N}\hat{w}\left(x_p,y_q\right)e^{-jk_x x_p}e^{-jk_y y_q}. \tag{1}$$

The inhomogeneous wave used in the inhomogeneous wave correlation is denoted $\hat{\sigma}_{k,\gamma,\theta}$, and corresponds to a propagating wave in the direction θ with an attenuation γ and a wavenumber k. It is defined as follows:

$$\hat{\sigma}_{k,\gamma,\theta}(x_p,y_q) = e^{-jk(\theta)(1+j\gamma(\theta))(x_p\cos(\theta)+y_q\sin(\theta))} \tag{2}$$

The correlation between this inhomogeneous wave and the measured wave field is therefore given by (see Ref. [21])

$$\mathrm{IWC}(k,\gamma,\theta) = \frac{\left|\frac{l_x l_y}{N^2}\sum_{p=1}^{N}\sum_{q=1}^{N}\hat{w}\left(x_p,y_q,\omega\right)\hat{\sigma}^{*}_{k,\gamma,\theta}\right|}{\sqrt{\frac{l_x l_y}{N^2}\sum_{p=1}^{N}\sum_{q=1}^{N}\hat{\rho}\left(x_p,y_q\right)\left|\hat{w}(x_p,y_q,\omega)\right|^2\sum_{p=1}^{N}\sum_{q=1}^{N}\hat{\rho}\left(x_p,y_q\right)\left|\hat{\sigma}_{k,\gamma,\theta}\right|^2}}, \tag{3}$$

where $*$ denotes the complex conjugate. The coherence function $\hat{\rho}(x_p, y_q)$ introduced in this equation is defined as the coherence between the input force and the measured displacement such as $\hat{\rho}\left(x_p, y_q\right) = \frac{|G_{fd}|^2}{G_{ff} G_{dd}}$ with G_{dd}, G_{ff} and G_{fd} the displacement autospectrum, the force autospectrum, and the force–displacement cross-spectrum respectively. The identification of the complex wavenumber in a given direction θ is obtained by maximizing IWC(k, γ, θ). This maximization is made on two levels. The real part $k(\theta)$ is first estimated, and the attenuation coefficient γ is then estimated around this estimation $k(\theta)$. The resulting complex wavenumber writes $\tilde{k}(\theta) = k(\theta)(1 + \mathrm{j}\gamma(\theta))$.

Using the method described above, the Damping Loss Factor is then determined at each frequency with the following relationship (see Ref. [14]):

$$\eta = \left| \frac{\mathrm{Im}(\tilde{k}^4)}{\mathrm{Re}(\tilde{k}^4)} \right|. \tag{4}$$

Finally an iterative refinement process is applied to minimize the error on the estimated Damping Loss Factor. This process is summarized in Algorithm 1. Note that this study is done in a statistical energy analysis framework where the damping loss factor anisotropy is not considered (contrary to the example presented in Ref. [25] showing the effect of anisotropy on the damping loss factor). Therefore only the global damping loss factor is presented in the following and compared with some reference methods.

Algorithm 1. Inverse Wave Method.

Evaluate the initial wavenumber and damping loss factor $k^0(\omega, \theta), \eta^0(\omega, \theta)$, and choose the search domain accordingly.
while Convergence isn't reached **do**
→ Refine the search domain around the current estimation of the wavenumber and damping loss factor: $k^n(\omega, \theta), \eta^n(\omega, \theta)$.
for each frequency ω **do**
for each angle of propagation θ
→ Calculate IWC with Eq. (3)
→ Calculate the new estimates with:
$k^{n+1}(\omega, \theta), \gamma^{n+1}(\omega, \theta) = \underset{k,\gamma}{\mathrm{argmax}}(\mathrm{IWC}(:, :, \theta))$,
$\eta^{n+1}(\omega, \theta) = 4\gamma^{n+1}(\omega, \theta)$.
end for
→ Apply a curve smoothing in angle and a weighting with the IWC on the new estimates.
end for
→ Apply a curve smoothing in frequency on the new estimates.
end while

3. Reference methods

In this section the classical methods used to estimate the structural damping are recalled.

3.1. Half-power bandwidth method (3 dB method)

This technique estimates the modal damping and is well adapted to low frequency (with a low modal overlap). Other modal testing methods, such as the multi-degree-of-freedom pole-residue fitting methods (see Ref. [26]), could be employed to reach higher frequencies but these methods are well beyond the scope of the present study. Therefore only the basic half-power bandwidth method is used in the current work as a validation when it is possible. For each resonance, the modal damping η_n is given by (see Ref. [7])

$$\eta_n = \frac{\Delta f}{f_n}, \tag{5}$$

where f_n is the resonance frequency of the mode and Δf the half-power bandwidth of the mode (-3 dB). This modal damping is compared with the band-averaged loss factor obtained with the other methods.

3.2. Decay rate method

The Decay Rate Method is based on the logarithmic decrement of the transient structural response. Accelerometers are placed on the plate to measure the decay of the vibrations after the excitation is cut off. Here the damping is assumed to have an exponential decay and the same damping is assumed for all the modes in the same frequency band (third-octave band here). The damping loss factor is then given, for a third-octave band with a decay rate DR (in dB/s), by the following expression (see Ref. [8]):

$$\eta_i = \frac{\mathrm{DR}}{27.3 f}. \tag{6}$$

3.3. Power input method

The power input method is directly derived from the Statistical Energy Analysis (SEA) power balance equation. The damping loss factor is obtained from the measurement of the power injected to the structure and the spatially averaged square velocity produced. In steady-state conditions, the space and frequency averaged input power is equal to the average dissipated power. The average loss factor writes then (see Ref. [9])

$$\eta_i = \frac{P_i}{\omega E_i}. \tag{7}$$

Here $P_i = 1/2\ \mathrm{Re}(F^* v) = 1/2\ \mathrm{Re}(\int_{\omega_1}^{\omega_2} G_{Fv}(\omega)\,\mathrm{d}\omega)$ is the input power obtained from the real part of the cross-spectral density $G_{Fv}(\omega)$ between the force F and the velocity v. Finally the space and frequency averaged total energy is calculated with $E_i = M_i v_i^2 = M_i \int_{\omega_1}^{\omega_2} G_{vv}(\omega)\,\mathrm{d}\omega$ where M_i is the mass related to the measurement area. It is calculated from the auto-spectral density, $G_{vv}(\omega)$, of the velocity signals output from the accelerometers. The input power and the total energy are both calculated on a third-octave band $[\omega_1, \omega_2]$. Following SEA best-practice in the implementation of the power input method, one must avoid excitation near an edge, responses points at short distances from the excitation point (direct field) and response points at large distances from the excitation (the responses may die-out as a result of relatively high damping and relatively long distances). In consequence, for each excitation, the measurements must be performed outside a circle centered on the source location with a radius R_D at which the kinetic energy of the direct field equals that of the reverberant field. This radius is calculated using (see Ref. [27])

$$R_D = \frac{\omega \eta h}{2\pi c_g}, \tag{8}$$

where η is the damping loss factor estimated with the 3 dB method, h is the thickness of the tested panels and c_g is the group velocity. The measurement area is therefore limited by an inner radius R_{D1} equal to 0.03 m (calculated with Eq. (8)), but also by an outer radius R_{D2} equal to three-fourths of the distance between the excitation and the nearest edge. These areas are shown in Fig. 6 for the tested panels. In this work, the panels were excited by a shaker fed with a white noise. The input power was measured using an impedance head and the response of the panels with classical accelerometers. The input power and quadratic velocities of the panels were averaged over 4 shaker locations. Quadratic velocities were space-averaged over 120 measurement locations.

4. Numerical validation

A numerical model is used to test the inverse wave method on a 2 mm thick aluminium panel (density $\rho = 2740\ \mathrm{kg/m^3}$, Young's modulus $E = 70E9(1+\eta\mathrm{j})\mathrm{Pa}$, Poisson Coefficient $\nu = 0.33$) of dimensions 1 m by 1 m with free boundary conditions. The plate is discretized with quadratic elements over a mesh with 80 elements by 80 elements. Three cases are tested with a structural damping of 1 percent, 5 percent and 10 percent respectively. Note that the area of calculation $l_x \times l_y$ is reduced of 30 percent on the edges when the damping loss factor is higher than or equal to 5 percent. In this case, the waves decrease quickly and are not significant over the full area $L_x \times L_y$. Note also that a constraint on the wavenumber based on a prior measurement can be efficiently applied to enhance the characterization of the damping.

Three examples of inhomogeneous wave correlation distribution in the wavenumber domain are presented in Fig. 1 at 1003 Hz with different damping coefficients. The plate displacements are calculated here with the previous numerical model and the inhomogeneous wave correlation results presented are obtained with the same damping coefficient in Eq. (3). The damping effect is well highlighted on these figures.

On the other hand, the corresponding estimated wavenumbers are plotted in Fig. 2. The wavenumbers are also estimated with Algorithm 1. The theoretical wavenumbers are well identified for the three tested damping ratios, and show the reliability and the accuracy of the method.

Finally, the estimated damping ratios are presented in Figs. 3–5. In particular, the damping ratio estimated from the numerical model results with 1 percent of structural damping is presented in Fig. 3. Three steps are necessary to converge. The first estimation is made between 0 percent and 20 percent and gives an estimated damping around 2 percent. The refined estimation is then made between 0 percent and 5 percent, and gives a good estimation of the damping around 1.3 percent. The final estimation is made between 0 percent and 3 percent and gives a very good estimation of the damping around the expected value of 1 percent.

The damping ratio estimated from the numerical model results with 5 percent of structural damping is presented in Fig. 4. Three steps are again used to converge. The first estimation is made between 0 percent and 20 percent, and leads to an estimated damping around 8–9 percent. The refined estimation is then made between 0 percent and 10 percent, and gives an estimation of the damping around 6 percent. The final estimation is made between 3 percent and 7 percent and gives a good estimation of the damping close to the expected 5 percent.

The damping ratio estimated from the numerical model results with 10 percent of structural damping is presented in Fig. 4. Three steps are again used to converge. The first estimation is made between 0 percent and 20 percent, and leads to an estimated damping around 7–10 percent. The refined estimation is then made between 5 percent and 15 percent, and

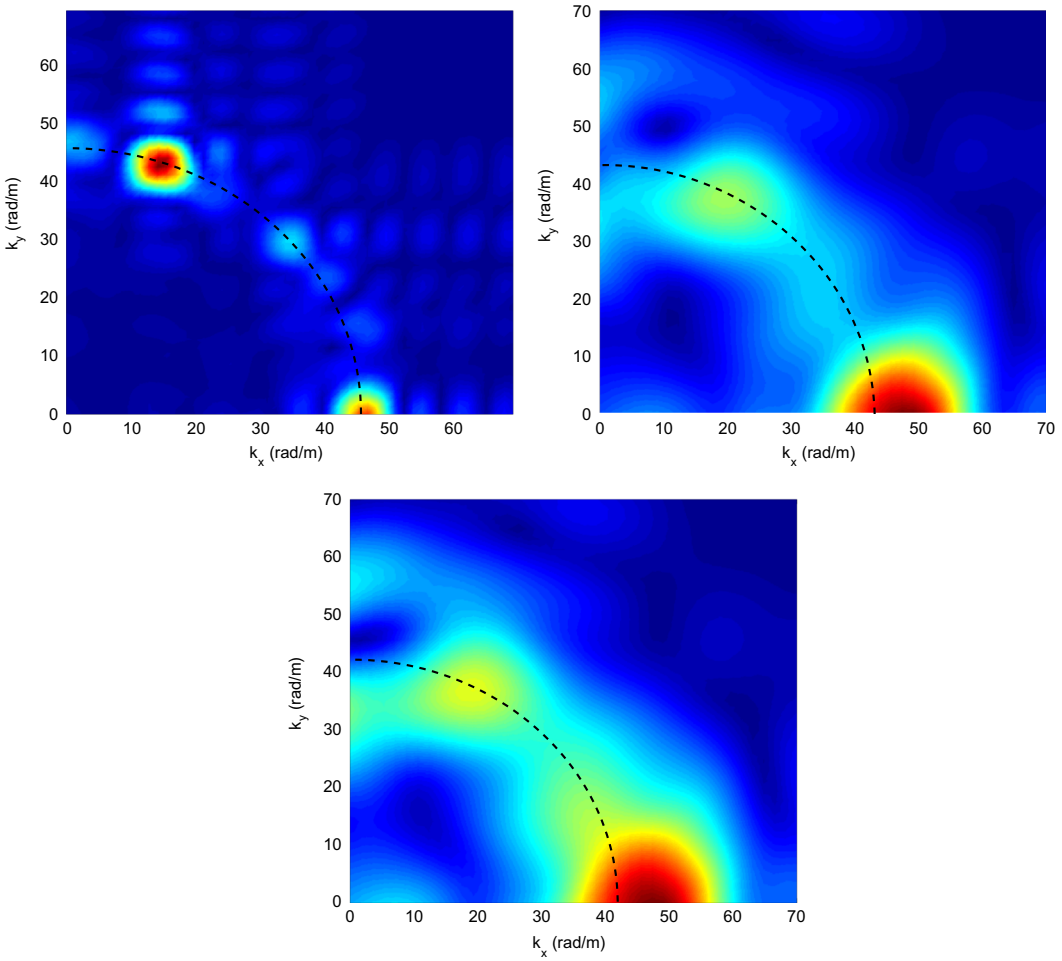

Fig. 1. Inhomogeneous Wave Correlation (IWC) of a plate at 1003 Hz obtained from a finite element model. - - - Estimated wavenumber. Top Left: 1% of structural damping, Top Right: 5% of structural damping, Bottom: 10% of structural damping.

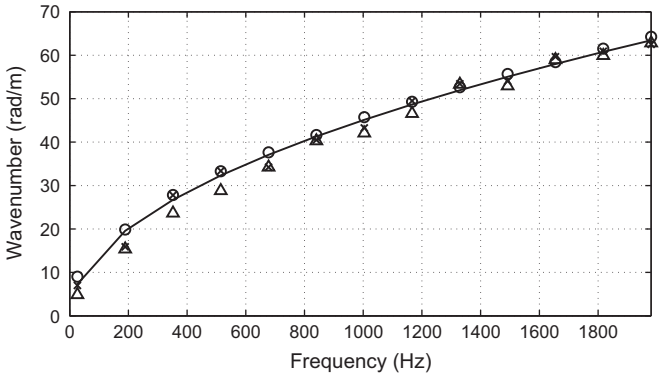

Fig. 2. Comparison between the theoretical wavenumber and the wavenumbers estimated with the Inverse Wave Method and a numerical model. — Theoretical wavenumber, ○ Inverse Wave Method estimation with 1% of structural damping, × with 5% of structural damping, ▵ with 10% of structural damping.

gives an estimation of the damping around 7–9 percent. The final estimation is made between 8 percent and 14 percent and gives a slightly underestimated damping around 9.5 percent. This last result shows the difficulty to estimate the damping of structures with a higher damping.

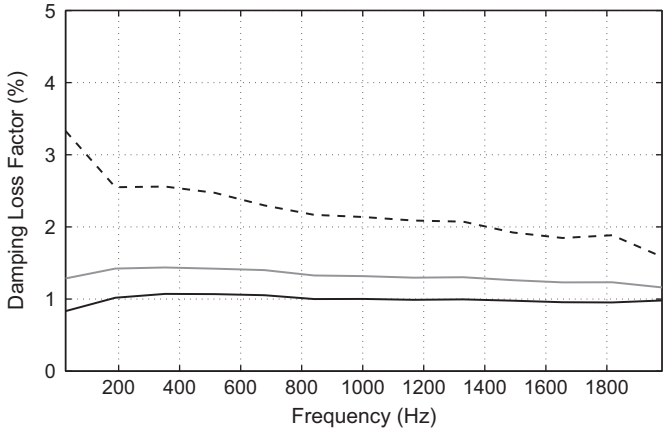

Fig. 3. Damping Loss Factor estimated with the Inverse Wave Method on a numerical model with 1% of structural damping: - - - first estimation between 0% and 20%, ═ refined estimation between 0% and 5%, ═ final estimation between 0% and 3%.

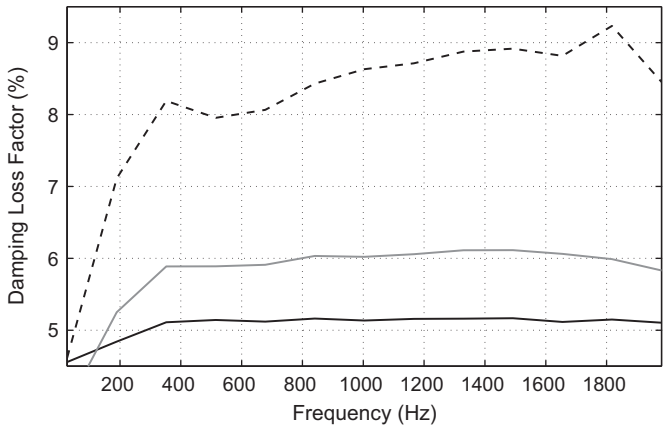

Fig. 4. Damping Loss Factor estimated with the Inverse Wave Method on a numerical model with 5% of structural damping: - - - first estimation between 0% and 20%, ═ refined estimation between 0% and 10%, ═ Final estimation between 3% and 7%.

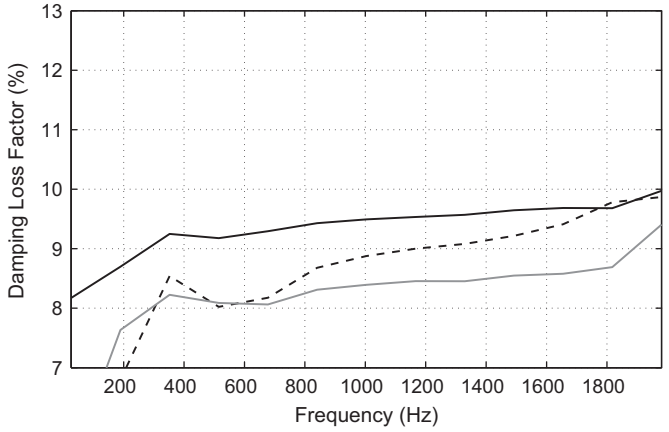

Fig. 5. Damping Loss Factor estimated with the Inverse Wave Method on a numerical model with 10% of structural damping: - - - first estimation between 0% and 20%, ═ refined estimation between 5% and 15%, ═ final estimation between 8% and 14%.

5. Experimental validation

This section describes the measurement setup used to estimate the damping loss factor of different panels. The analysis is performed in a large frequency band between 100 Hz and 10 kHz. An isotropic aluminium panel and two aircraft

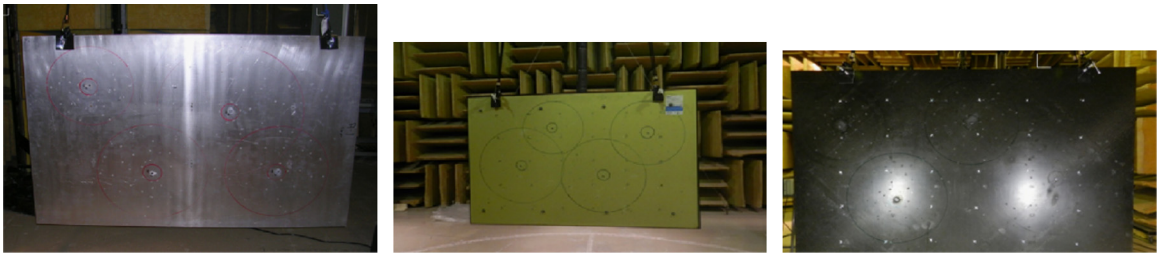

Fig. 6. Three tested panels: one aluminium panel and two composite panels.

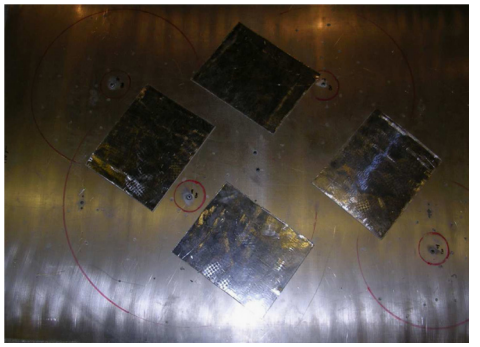

Fig. 7. Aluminium panel treated with viscoelastic patches.

Table 1
Characteristics of the materials.

	Thin skins	Thin core	Thick skins	Thick core
h (mm)	0.96	25.4	0.51	6.35
E_1 (MPa)	46×10^3	1	23.6×10^3	0.001
E_2 (MPa)	46×10^3	1	23.6×10^3	0.001
E_3 (MPa)	46×10^3	179	23.6×10^3	138
G_{12} (MPa)	17.6×10^3	1	10.34×10^3	1
G_{12} (MPa)	17.6×10^3	26	10.34×10^3	44.8
G_{13} (MPa)	17.6×10^3	56	10.34×10^3	24.1
ν_{12}	0.3	0.45	0.141	0.45
ν_{12}	0.3	0.01	0.141	0.01
ν_{13}	0.3	0.01	0.141	0.01
ρ (kg/m^3)	1900	64	1900	48

composite panels are studied (see Fig. 6), including a thin panel representative of a trim panel and a thick panel representative of a skin or floor panel. Both composite panels are made of a Honeycomb (HC) core and two identical isotropic skins. Two levels of comparison with full experimental data are used in this validation. The first aims to roughly check the method on an isotropic homogeneous aluminium plate. The second aims to test the method on more complex panels. In order to validate the methodology with a highly damped panel, patches of viscoelastic constrained layer were also added to the aluminum panel. This test is performed with 20 percent coverage area (see Fig. 7). The material was bonded only on one surface of the panel. All the panels have a surface area equal to 1.5 m^2 ($L_x = 1.5$ m, $L_y = 1$ m). The thicknesses of the aluminium panel and the two composite panels are 2 mm, 26.4 mm and 6.8 mm, respectively. The detailed properties of the sandwich composite panels are given in Table 1.

In the following measurements, the panels were freely hung with flexible cords in a semi-anechoic room (Fig. 7). A shaker was attached at the center of the panel and was driven by a broadband white noise signal. The input force was measured with a force sensor. A scanning laser vibrometer was used to measure the velocity over a surface mesh. A scan area of 0.8 m by 0.8 m was used with 80 points along the X direction and 80 points along the Y direction for a total of 6400 measurement points. Measuring the plate response, $\hat{w}(x_p, y_q)$, at each point of the scanning area and using the transform to the wavenumber space leads to the flexural wavenumber (see Eq. (1)). The technique is restricted by the size of the scan area and requires equally spaced measurement.

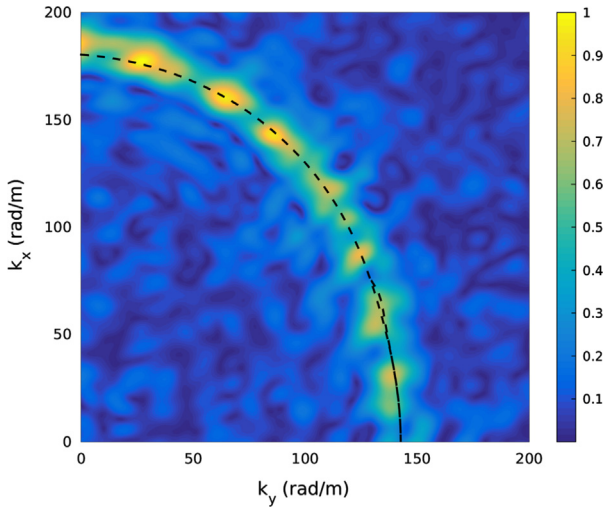

Fig. 8. Inhomogeneous Wave Correlation (IWC) of the thin composite panel at 8250 Hz: - - - identified wavenumber.

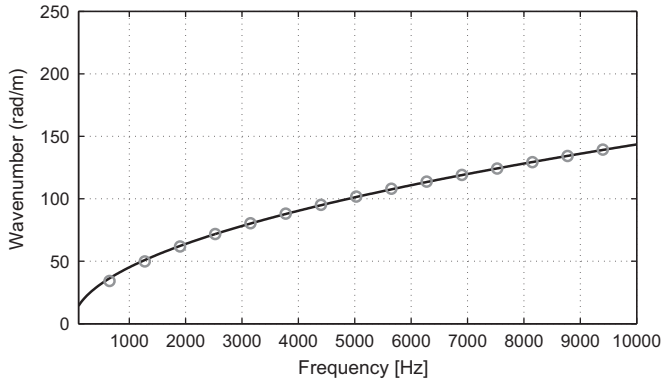

Fig. 9. Dispersion curve of an aluminium panel. Theoretical wavenumber (——) vs measured wavenumber with the inverse wave correlation method (○).

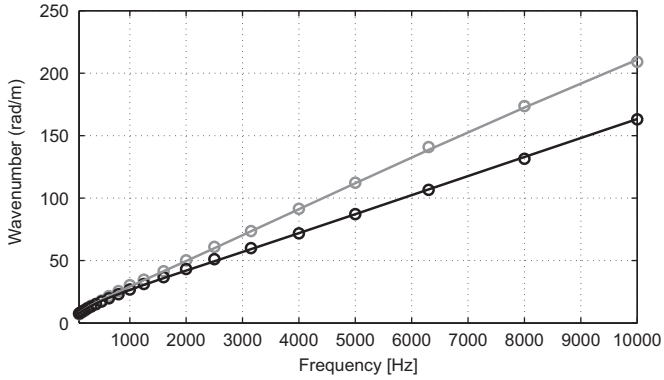

Fig. 10. Dispersion curve of the thin composite panel. Theoretical wavenumbers in the directions k_x (——) and k_y (——) vs measured wavenumbers with the inverse wave correlation measurements in the same directions k_x (○) and k_y (○).

5.1. Wavenumber estimation

The estimated wavenumbers for the isotropic aluminum panel, the thin and the thick composite sandwich panels are shown in Figs. 9, 10 and 11 respectively. For each panel, the wavenumber curves measured along the *X* and *Y* directions using the correlation technique are compared with the thin plate theory for the aluminum isotropic panel and with a General Laminate Model (GLM) [28] for the composite sandwich panels. An example of experimental inhomogeneous wave

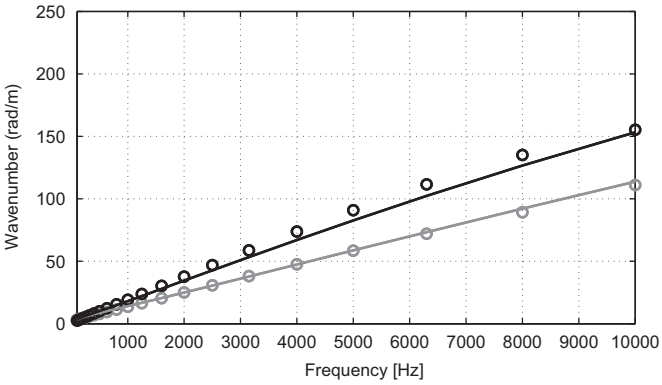

Fig. 11. Dispersion curve of the thick composite panel. Theoretical wavenumbers in the directions k_x (——) and k_y (——) vs measured wavenumbers with the inverse wave correlation measurements in the same directions k_x (○) and k_y (——).

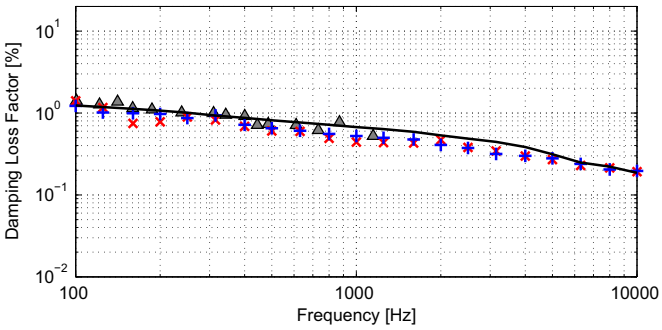

Fig. 12. Experimental damping loss factors measured on the isotropic aluminium panel with the 3 dB method (▲), the decay rate method (+), the power input method (✕), and the inverse wave correlation method (——).

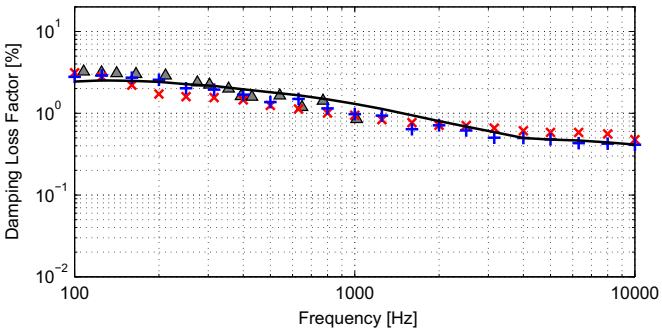

Fig. 13. Experimental damping loss factors measured on the isotropic aluminium panel treated with viscoelastic patches with the 3 dB method (▲), the decay rate method (+), the power input method (✕), and the inverse wave correlation method (——).

correlation distribution for the thin composite sandwich panel at 8250 Hz is presented in Fig. 8 where the orthotropic behavior is visible and identifiable.

Overall, the comparison between the experimental and analytical results is good for all the panels. At high frequency, the correlation technique gives a good estimation due to fine mesh used in the scan. However, small differences are observed in the *Y* direction for the thick panel between the measured and the theoretical values (see Fig. 11). This may be due to uncertainties on the panel mechanical properties given by the manufacturer.

5.2. Damping loss factor estimation

A comparison between damping loss factors estimated with the half-power bandwidth method (−3 dB), the decay rate method, the power input method and the inverse wave method is presented in Figs. 12–15. The half-power bandwidth method (−3 dB) results are used only as a validation tool when applicable (visible modes).

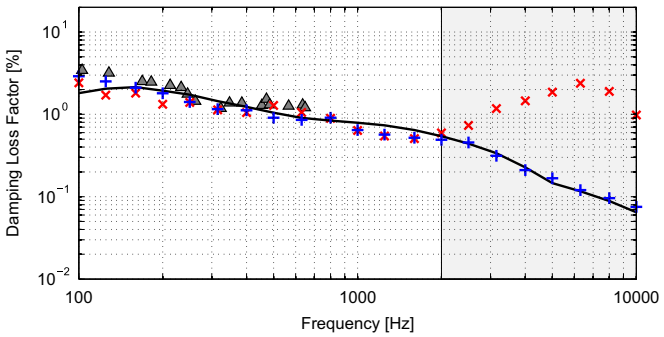

Fig. 14. Experimental damping loss factors measured on the thin composite panel with the 3 dB method (▲), the decay rate method (+), the power input method (×), and the inverse wave correlation method (—).

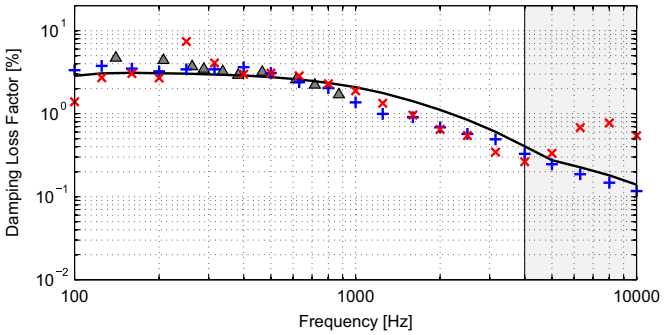

Fig. 15. Experimental damping loss factors measured on the thick composite with the 3 dB method (▲), the decay rate method (+), the power input method (×), and the inverse wave correlation method (—).

For the aluminium panel with and without the viscoelastic patches, the damping influence is clearly visible in Figs. 12 and 13. The estimations of the damping loss factor correlate well with the increase of damping. A good comparison between the different measurement methods is also obtained on these two cases. In particular the proposed Inverse Wave Method compares well with all the standard measurement methods.

For the two composite sandwich panels, the decay rate method, the power input method and the inverse wave method agree well at mid frequencies. At low frequency, i.e. around [100–300] Hz, the power input method presents some discrepancies compared to the other methods. The reason is the low number of modes at these frequencies. At high frequency, the damping loss factor estimated with the decay rate method and the inverse wave method is in good agreement. Meanwhile, the power input method is not able to estimate accurately the damping (see the gray area in Figs. 14 and 15). This is due to an experimental limitation in injecting the power to the system in this frequency region.

To sum up, an excellent comparison is obtained for all the panels using the inverse wave method thanks to the refined measurement scan used. However, the method seems less accurate at low frequencies, especially for the composite sandwich panels. This is usually a consequence of the size of the physical scan area, i.e. the bending wave length is too large to be captured at low frequencies.

6. Conclusions

This paper presents an Inverse Wave Method to estimate the damping loss factor of complex structures in two dimensions from a displacement field measured with a scanning laser vibrometer. The proposed technique estimates the flexural wavenumber and the damping loss factor of complex panels. A numerical model has first been used to test the proposed method and the feasibility of the method has been demonstrated. Then the method has been compared with three classical methods: the half-power bandwidth method, the Decay Rate Method and the steady-state Power Input Method. The experimental results, obtained with different panels, have once again shown the accuracy and the reliability of the proposed Inverse Wave Method to estimate both the wavenumber and the damping loss factor.

Acknowledgments

The authors would like to acknowledge Walid Kaffel, from the Polytechnic School of Tunisia, for his technical assistance, and Bombardier Aerospace for their composite panels.

References

[1] S. Assaf, M. Guerich, P. Cuvelier, Vibration and damping analysis of plates with partially covered damping layers, *Acta Acustica united with Acustica* 97 (4) (2011) 553–568.
[2] W. Palm, *Mechanical Vibrations*, John Wiley, Hoboken, NJ, 2007.
[3] E. Rivin, *Stiffness and Damping in Mechanical Design*, CRC Press, New York, 1999.
[4] A. Nashif, D. Jones, J.P. Henderson, *Vibration Damping*, John Wiley, New York, 1985.
[5] S. Rao, Mechanical Vibrations, 5th edition, 2010, Prentice Hall, Pearson PLC.
[6] C. Fuller, S. Elliott, P. Nelson, *Active Control of Vibration*, 1st edition, Academic Press, London, 1997.
[7] G. Papagiannopoulos, G. Hatzigeorgiou, On the use of the half-power bandwidth method to estimate damping in building structures, *Soil Dynamics and Earthquake Engineering* 31 (7) (2011) 1075–1079.
[8] B.C. Bloss, M.D. Rao, Estimation of frequency-averaged loss factors by the power injection and the impulse response decay methods, *The Journal of the Acoustical Society of America* 117 (1) (2005) 240–249.
[9] D. Bies, S. Hamid, in situ determination of loss and coupling loss factors by the power injection method, *Journal of Sound and Vibration* 70 (2) (1980) 187–204.
[10] Y. Liao, V. Wells, Estimation of complex Young's modulus of non-stiff materials using a modified Oberst beam technique, *Journal of Sound and Vibration* 316 (1–5) (2008) 87–100.
[11] E. Zhang, J. Chazot, J. Antoni, M. Hamdi, Bayesian characterization of Young's modulus of viscoelastic materials in laminated structures, *Journal of Sound and Vibration* 332 (16) (2013) 3654–3666.
[12] J.-D. Chazot, B. Nennig, A. Chettah, Harmonic response computation of viscoelastic multilayered structures using a zpst shell element, *Computers and Structures* 89 (23–24) (2011) 2522–2530.
[13] F. Ablitzer, C. Pezerat, J.-M. Genevaux, J. Begue, Identification of stiffness and damping properties of plates by using the local equation of motion, *Journal of Sound and Vibration* 333 (9) (2014) 2454–2468.
[14] J. McDaniel, P. Dupont, L. Salvino, A wave approach to estimating frequency-dependent damping under transient loading, *Journal of Sound and Vibration* 231 (2) (2000) 433–449.
[15] N. Ferguson, C. Halkyard, B. Mace, K. Heron, The estimation of wavenumbers in two-dimensional structures, 2002, pp. 799–806.
[16] K. Grosh, E.G. Williams, Complex wave-number decomposition of structural vibrations, *The Journal of the Acoustical Society of America* 93 (2) (1993) 836–848.
[17] J. Berthaut, M. Ichchou, L. Jezequel, K-space identification of apparent structural behaviour, *Journal of Sound and Vibration* 280 (3–5) (2005) 1125–1131.
[18] M. Ichchou, J. Berthaut, M. Collet, Multi-mode wave propagation in ribbed plates: *part i, wavenumber-space characteristics*, *International Journal of Solids and Structures* 45 (5) (2008) 1179–1195.
[19] M. Ichchou, J. Berthaut, M. Collet, Multi-mode wave propagation in ribbed plates—part ii: *predictions and comparisons*, *International Journal of Solids and Structures* 45 (5) (2008) 1196–1216.
[20] M. Ichchou, O. Bareille, J. Berthaut, Identification of effective sandwich structural properties via an inverse wave approach, *Engineering Structures* 30 (10) (2008) 2591–2604.
[21] M. Rak, M. Ichchou, J. Holnicki-Szulc, Identification of structural loss factor from spatially distributed measurements on beams with viscoelastic layer, *Journal of Sound and Vibration* 310 (4–5) (2008) 801–811.
[22] C. Halkyard, Maximum likelihood estimation of flexural wavenumbers in lightly damped plates, *Journal of Sound and Vibration* 300 (1–2) (2007) 217–240.
[23] A. Thite, N. Ferguson, Wavenumber Estimation: Further Study of the Correlation Technique and Use of SVD to Improve Propagation Direction, Resolution, Technical Report 937, ISVR Technical Memorandum, 2004.
[24] R. Cherif, N. Atalla, Experimental investigation of the accuracy of a sandwich model, *Journal of the Acoustical Society of America* 137 (3) (2015) 1541–1550.
[25] S. Ghinet, N. Atalla, Modeling thick composite laminate and sandwich structures with linear viscoelastic damping, *Computers and Structures* 89 (15-16) (2011) 1547–1561.
[26] D. Ewins, Modal Testing: Theory, Practice and Application, 2nd edition, Wiley-Blackwell, 2000.
[27] R. Lyon, R. DeJong, *Theory and Application of Statistical Energy Analysis*, Butterworth-Heineman, Boston, USA, 1995.
[28] S. Ghinet, N. Atalla, H. Osman, Diffuse field transmission into infinite sandwich composite and laminate composite cylinders, *Journal of Sound and Vibration* 289 (4–5) (2006) 745–778.